International Journal of Microwave and Wireless Technologies, 2010, 2(6), 531–536.
doi:10.1017/S1759078710000760

Novel designs of polarization-preserving circular waveguide filters

JENS BORNEMANN AND SENG YONG YU

Novel designs of circular waveguide components for lowpass, highpass, bandpass, and bandstop applications are presented. The filters are formed by cascaded TM_{11}-mode resonator sections which share a common axis, thus preserving the polarizations of input signals due to rotational symmetry. Moreover, the filters are smaller than standard TE_{11}-mode bandpass filters. Basic design considerations are discussed with respect to the connection of TM_{11}-mode resonators through circular irises. Design principles for all four filter types are presented and their performances computed by the coupled-integral equation technique (CIET). All filter performances are verified by the commercially available software package μWave Wizard, and structural dimensions are provided.

Keywords: Circular waveguide filters, Lowpass filters, Highpass filters, Bandpass filters, Bandstop filters, Computer-aided design, Circular waveguide modes, Polarization

Received 2 March 2010; Revised 13 September 2010

I. INTRODUCTION

In order to preserve the polarization of signals, waveguide circuits are required to have a common center axis, and they must conform to the following conditions: Each cross section must be two-plane symmetric, such as in quadruple-ridged waveguides [1, 2] or in orthomode horn applications [3–5]. Alternatively, the entire component can possess rotational symmetry, e.g. [6–9]. Both features benefit from extended bandwidth, e.g. [4, 7], through the excitation of only those modes that satisfy structural symmetry along with that of the incoming electromagnetic field, e.g. [8, 9].

Modern microwave filters are required to possess properties such as wide bandwidth, improved out-of-band performance, the ability to generate transmission zeros, and preservation of all polarizations. Although the mechanism to generate transmission zeros at finite frequencies in the filter response is well understood in standard dual-mode filters, e.g. [10, 11], fulfilling the polarization-preserving specifications is not necessarily a straightforward design exercise, e.g. [12].

Recently, inline rectangular waveguide filters have been proposed which utilize the resonances of TM_{11} modes to create filters and the fundamental-mode TE_{10}-mode bypass coupling to generate transmission zeros [13]. Unfortunately, this design does not lend itself to two-plane cross-section symmetry due to the mandatory offsets between connected waveguides. The equivalent scenario in circular waveguide technology would employ TM_{01}-mode resonators. However, the TM_{01} will not be excited by an axial symmetric connection to the fundamental TE_{11} mode of a circular waveguide. (The reader is referred to [14] for plots of modal field distributions in rectangular and circular waveguides.)

Therefore, we utilize the circular waveguide TM_{11} mode to create an equivalent to the so-called singlet design in rectangular waveguide [13]. It will be demonstrated in this paper that this approach leads to the design of rotationally symmetric, thus polarization-preserving, circular waveguide filters and allows the creation of transmission zeros. Moreover, a bandpass filter using TM_{11}-mode resonators will be much shorter than one realized with conventional TE_{11}-mode cavities.

This work is an extension of [15] but it incorporates a number of additional aspects. First, we will explain the fundamental connections between TM_{11}-mode resonators and their adjacent circular waveguide sections. Different scenarios are discussed which will later be exploited for the design of lowpass, highpass, bandpass, and bandstop filters. We also demonstrate the limiting aspect of TM_{01}-mode resonators as opposed to TM_{11}-mode resonators. Finally, examples of bandstop and lowpass filters are added which demonstrate that the entire range of filter categories can be designed to preserve polarization of the filtered signals.

II. DESIGN CONSIDERATIONS

For the purpose of initiating the discussion with respect to an individual filter category, we start with a regular circular waveguide iris filter that is straightforwardly designed using cascaded half-wave cavities separated by irises that act as impedance inverters [16, 17]. The inset of Fig. 1 shows the filter which is designed for a center frequency of 11.5 GHz, a bandwidth of 500 MHz, and a return loss of 22 dB. Stopband requirements were selected such that seven cascaded TE_{11}-mode cavities are obtained. This filter is used as a first prototype to satisfy the demand for the preservation of polarization. WC 80 (20.24 mm in diameter) input and output waveguides are selected and are maintained

Department of Electrical and Computer Engineering, University of Victoria, PO Box 3055, Victoria, BC V8W 3P6, Canada.
Corresponding author:
J. Bornemann
Email: j.bornemann@ieee.org

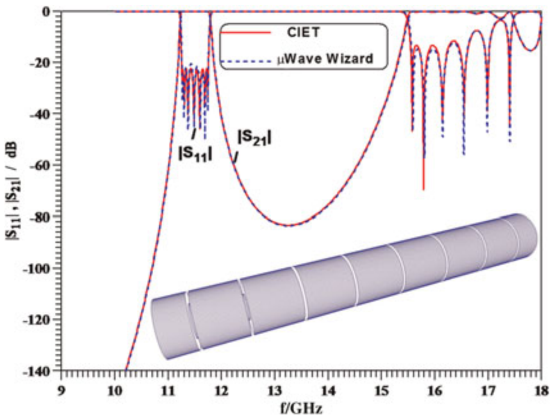

Fig. 1. Performance of a seven-resonator regular circular waveguide iris filter designed for 500 MHz bandwidth at 11.5 GHz (cf. Table 1).

throughout the paper for better comparison between filters or filter components. The fundamental TE_{11}-mode cutoff frequency of the ports is 8.68 GHz. Due to rotational symmetry, the next excited higher order mode is TM_{11} with a cutoff frequency of 18.1 GHz. Thus, the operational bandwidth under consideration of rotational symmetry is about 9–18 GHz. Similar principles are applied in other on-axis connected circular waveguide components such as, e.g., corrugated horns [7]. The cutoff frequencies of the two modes involved in this work are

$$f_{cTE_{11}} = 1.8412\frac{c}{\pi d}, \quad f_{cTM_{11}} = 3.8317\frac{c}{\pi d}, \qquad (1)$$

where c is the speed of light and d is the diameter of the waveguide.

Figure 1 shows the performance of the regular circular waveguide iris filter. Its length from first to last iris is 131.5 mm with 1 mm thick irises (cf. Table 1). It is observed that the main passband is well represented but a second wider passband appears already at 15.5 GHz, thus limiting the applicable bandwidth of such a design.

In order to improve the stopband performance, the use of frequency-dependent radial inverters was suggested [3] as they are capable of adding transmission zeros in the lower and/or upper stopband of a bandpass filter. As is demonstrated in [3, 15], however, the introduction of such transmission zeros fails to prevent the second passband due to the fact that the electrical lengths of the resonators remain largely unchanged.

In order to eliminate the second passband in Fig. 1 or move any higher-order resonances beyond 18 GHz, shorter cavities must be used whose resonances are independent of length. This is possible by using resonating TM_{mno} modes. As pointed out earlier, the TM_{010} mode will not be excited by a rotationally symmetric connection to a fundamental-mode circular waveguide. Therefore, we are investigating in Fig. 2 the use TM_{110}-mode cavities. In all three cases, the cavity has a diameter of 36 mm and a length of 2 mm. These dimensions have purposely been selected to provide a resonance that is lower than the passband in Fig. 1. It will aid in demonstrating in Fig. 3 the limitations of an offset-connected TM_{010}-mode resonator.

Figure 2(a) shows a direct connection between the TM_{110}-mode cavity and WC 80 waveguides whose TE_{11}-mode cutoff frequency is at 8.68 GHz. The resonator

Table 1. Dimensions of circular waveguide filters (diameters d_n and lengths l_n in mm).

	Fig. 1	Fig. 4	Fig. 6	Fig. 7	Fig. 8
d_0	20.240	20.240	20.240	20.240	20.240
l_0	10.000	10.000	10.000	10.000	10.000
d_1	12.185	12.522	17.444	33.489	24.860
l_1	1.000	0.500	10.540	1.217	2.980
d_2	20.244	29.838	34.472	19.524	20.003
l_2	16.043	4.940	1.198	5.579	4.300
d_3	9.419	9.877	15.818	32.331	25.596
l_3	1.000	0.500	6.167	3.856	3.774
d_4	20.244	29.813	30.565	19.485	19.872
l_4	18.057	4.018	2.834	2.950	2.268
d_5	8.673	8.015	13.049	31.702	25.184
l_5	1.000	0.500	0.972	5.728	3.110
d_6	20.244	30.272	29.639	18.278	20.122
l_6	18.423	3.176	4.950	1.904	1.452
d_7	8.518	7.082	12.981	31.274	26.348
l_7	1.000	0.500	2.009	6.266	3.516
d_8	20.244	30.490	29.604	18.278	20.765
l_8	18.478	3.103	5.637	1.904	2.703
d_9	8.518	7.082	12.981	31.702	27.836
l_9	1.000	0.500	2.009	5.728	3.555
d_{10}	20.244	30.272	29.639	19.485	20.949
l_{10}	18.423	3.176	4.950	2.950	3.012
d_{11}	8.673	8.015	13.049	32.331	26.630
l_{11}	1.000	0.500	0.972	3.856	5.265
d_{12}	20.244	29.813	30.565	19.524	20.363
l_{12}	18.057	4.018	2.834	5.579	3.241
d_{13}	9.419	9.877	15.818	33.489	27.890
l_{13}	1.000	0.500	6.167	1.217	3.565
d_{14}	20.244	29.838	34.472	20.240	19.949
l_{14}	16.043	4.940	1.198	10.000	1.213
d_{15}	12.185	12.522	17.444		27.739
l_{15}	1.000	0.500	10.540		6.215
d_{16}	20.244	20.240	20.240		19.863
l_{16}	10.000	10.000	10.000		1.402
d_{17}					28.410
l_{17}					3.911
d_{18}					20.240
l_{18}					10.000

produces as notch at 10.15 GHz similar to an E-plane stub in a rectangular waveguide. The resonance close to the cutoff frequency occurs due to the fact that at and close to cutoff, all sections support fundamental-mode propagation. This is also known from rectangular waveguide lowpass [16] and bandpass filters [18].

The basic shape of the curve in Fig. 2(a) implies that this direct connection can be exploited for either lowpass or bandstop filter applications. In the progress of connecting the TM_{110}-mode cavity to the input/output guides through irises, Fig. 2(b) shows coupling through a large iris. Compared to Fig. 2(a), we observe that the resonance close to cutoff vanishes as the iris prevents propagation at or close to cutoff. The notch frequency in Fig. 2(a) moves downwards to 9.45 GHz due to the fact that the irises contribute to the notch effect. A new resonance appears at 9.85 GHz. Moreover, another resonance (towards 12.5 GHz and beyond) might possibly be exploited for highpass applications.

As coupling through the irises decreases (Fig. 2(c)), the TM_{110}-mode resonance becomes more pronounced (9.62 GHz), and the notch frequency moves down to 9.2 GHz. This is the basic shape required for bandpass filters.

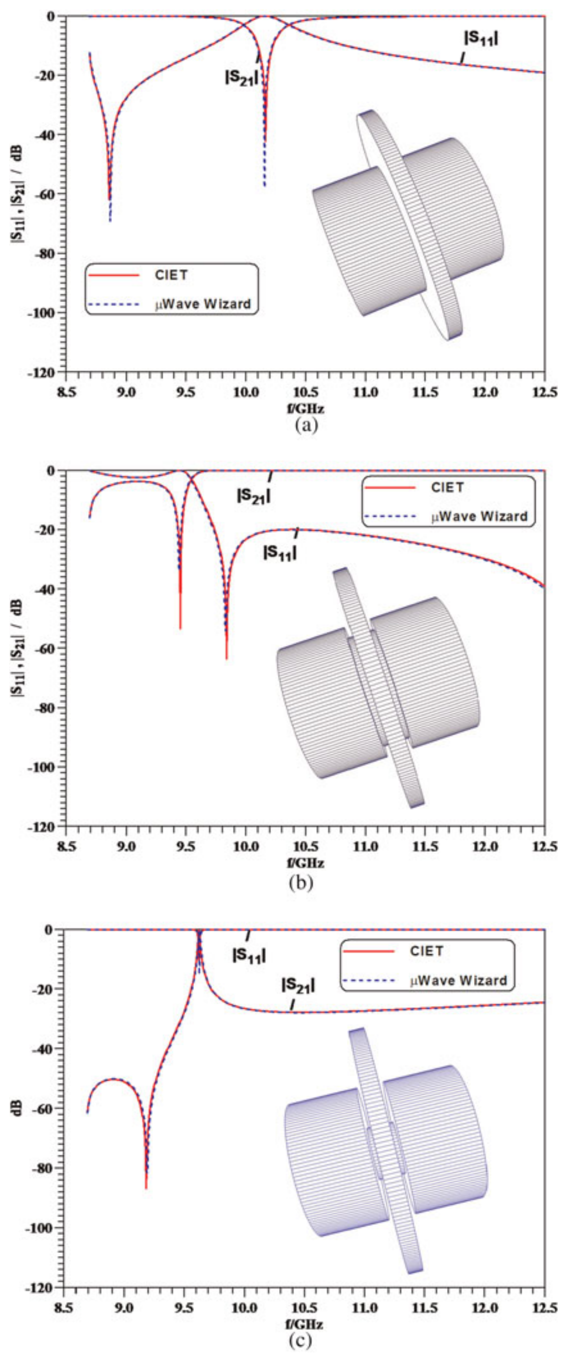

Fig. 2. Performance of a TM_{110}-mode cavity coupled to standard circular WC 80 waveguides: (a) direct coupling, (b) through large irises, and (c) through small irises.

For a bandpass filter designer, the question as to whether the transmission zero in Fig. 2(c) can be moved from being below to above the resonance is of fundamental importance. The answer is negative if rotational symmetry is to be maintained. Since the structure in Fig. 2(c) represents a singlet [13], the transmission zero is generated by a bypass coupling of the TE_{11} mode through the TM_{110}-mode resonator. Note that the cavity is too short for the TE_{11} mode to resonate. In order to move the transmission zero to the other side, the polarity of the main resonator must be reversed [13]. However, this is only possible if the feeding waveguide is moved off the center of the cavity. Figure 3 shows such a

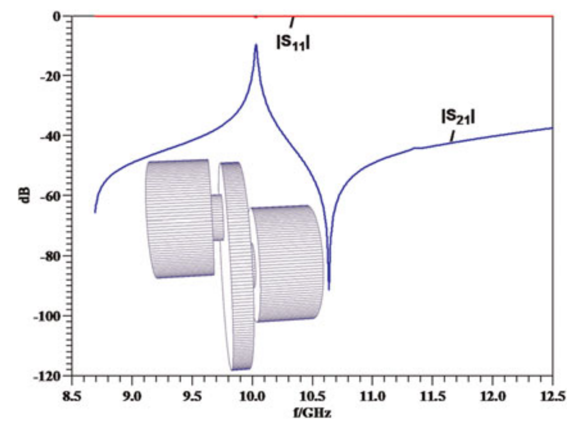

Fig. 3. μWave Wizard computation of an offset-connected TM_{010}-mode cavity with the transmission zero to the right of the resonance.

structure and its performance. Indeed, the transmission zero appears on the right side of the resonance. However, the resonating mode is no longer a pure TM_{110} but a combination of modes including the TM_{01} mode, which is excited due to the off-center connection. The cutoff frequency of the TM_{01} mode is

$$f_{cTM_{01}} = 2.405 \frac{c}{\pi d} \tag{2}$$

and it will propagate in the input/output ports above 11.34 GHz, thus severely limiting the operational bandwidth in addition to the loss of the polarization-preserving property of the filter.

For the design of rotationally symmetric circular waveguide filters, a coupling matrix approach according to [13] can be used in principle. However, it was experienced that the repeated computations of direct and bypass couplings for each resonator required large amount of manually input data. Therefore, the respective scenarios of Fig. 2 are selected for the filter characteristic at hand, and optimized [19] to satisfy a predefined response. The computational speed of the coupled-integral equation technique (CIET) permits the filter design to be completed within normal time frames. For instance, the analysis of the filter in Fig. 4 with 500 frequency points, TE/TM_{1n} modes up to 1000 GHz and TE/TM_{1n}-mode basis functions up to 200 GHz requires 8 s on a dual-core 1.66 GHz PC with 2 GB of RAM.

III. RESULTS

In order to compare a bandpass filter based on TM_{11}-mode cavities with the standard circular-iris filter displayed in Fig. 1, we use the properties displayed in Fig. 2(c) and cascade seven such resonators. Figure 4(a) shows the filter structure and its performance including comparison obtained with the μWave Wizard. Several differences are noted when comparing this response with that of Fig. 1. We obtain seven transmission zeros below the passband according to Fig. 2(c). The transition from stopband to passband between 11 and 11.25 GHz is significantly improved due to the appearance of the transmission zeros. This comes at the expense of a reduced stopband performance immediately above the passband. However, this apparent disadvantage is offset by the elimination of the second passband in Fig. 1 (15.5–18 GHz), where the filter in Fig. 4(a) maintains an attenuation of

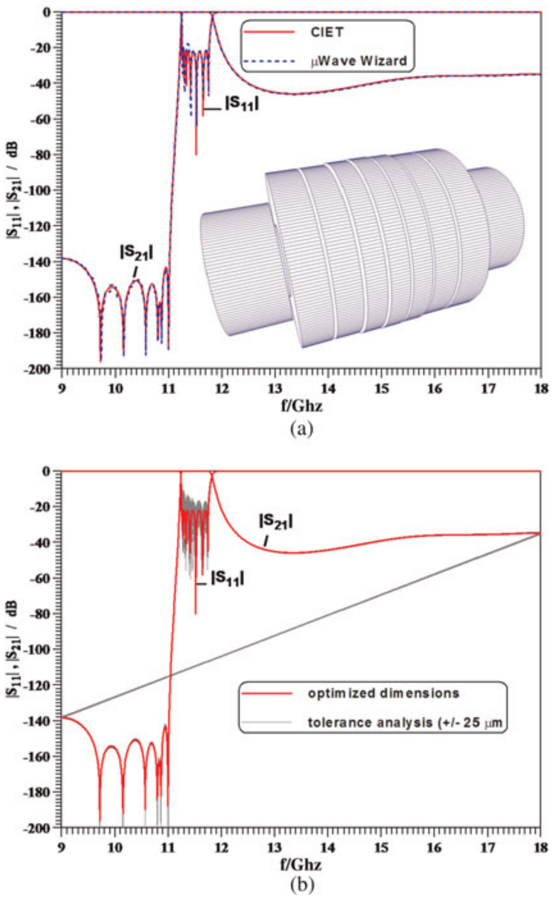

Fig. 4. Performance of a seven-resonator TM_{11}-mode filter (Table 1) for comparison with Fig. 1: (a) *S* parameters and (b) tolerance analysis.

35 dB. Note that the nearly constant attenuation level towards higher frequencies is in accordance with filter theory since all possible transmission zeros appear below the passband. Finally, the TM_{11}-mode filter in Fig. 4(a) is considerably more compact as its length from first to last iris is only 31.4 mm (cf. Table 1) – a reduction by more than 75% compared to the filter in Fig. 1.

The practical filter designer is, of course, concerned about accuracy of fabrication and tolerances involved in the process. Therefore, Fig. 4(b) shows a tolerance analysis of this filter. One hundred trials with variations of up to ± 25 μm are performed and plotted as thin gray lines in Fig. 4(b). It is demonstrated that the stopband performance displays a negligible influence on manufacturing tolerances of ± 25 μm and that the passband return loss variations are well within the margins of tolerance analyses performed in [20]. It is thus apparent that this filter (and the ones presented later in this paper) is subject to the same dependencies for mass production as other filters with or without transmission zeros [20].

Another advantage of utilizing TM_{11}-mode resonators becomes apparent when further investigating the capabilities of the singlet shown in Fig. 2(b). By increasing the length of the resonator as well as the diameters and lengths of the connected irises, two more resonances, which appear above that of the TM_{11} mode can be exploited. This is shown in Fig. 5, where the $|S_{11}|$ minimum at 11.41 GHz is due to the TM_{110} resonance. The TE_{11}-mode resonance in the iris causes the dip at 13.5 GHz, and that at 16.5 GHz is due to the TE_{111} resonance in the large cavity. Consequently, such a combination of axially connected circular waveguide sections is destined for quasi-highpass applications.

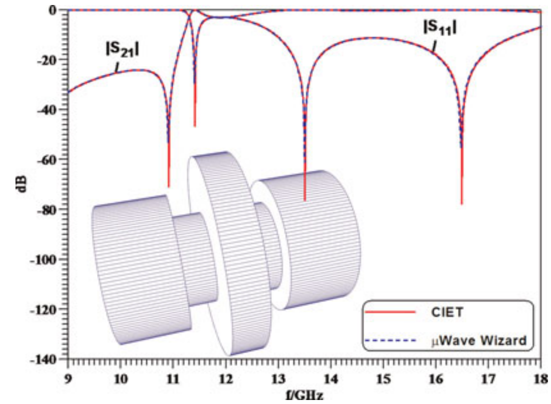

Fig. 5. Performance of an extended TM_{110}-mode singlet incorporating resonances of irises and that of the TE_{111} mode.

Based on this investigation, a quasi-highpass configuration formed by seven TM_{11}-mode resonators is assembled and optimized for a roll-off frequency of 11.21 GHz and return loss of 24 dB. The filter is shown in Fig. 6 (inset) together with its performance. The length including input and output irises is 63 mm and thus about twice as long as the bandpass filter depicted in Fig. 4. Note that rotational symmetry and thus polarization preservation has not been compromised.

For comparison with measurements the reader is directed to [21] where a comparable quasi-highpass filter in rectangular waveguide technology has been presented. The excellent agreement between measurements and CIET results in [21] as well as the verification of the filter response in Fig. 6 by the μWaveWizard validates the design procedure for polarization-preserving circular waveguide TM_{11}-mode filters.

Figures 4 and 6 demonstrate bandpass and highpass performances, respectively, of rotationally symmetric circular waveguide components. The up-to-now missing filter categories are bandstop and lowpass filters. According to Fig. 2(a), sandwiching a TM_{110}-mode resonator between two fundamental-mode circular waveguides produces a frequency notch. In order to obtain a narrow stopband and, at the same time, maintain an acceptable return loss (e.g. 20 dB) in the rest of the frequency range, a number of TM_{110}-mode cavities with

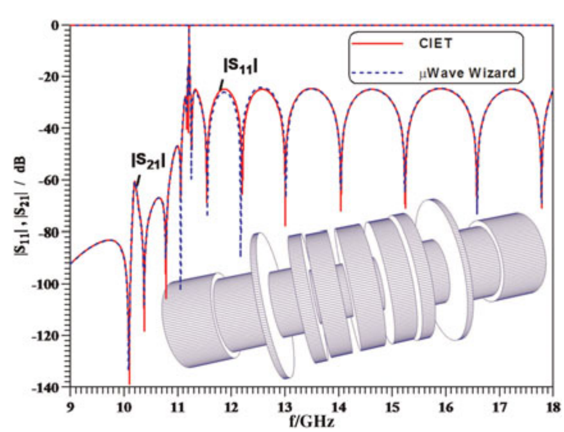

Fig. 6. Performance of a quasi-highpass filter (Table 1) with seven TM_{110}-mode resonators and additional resonances according to Fig. 5.

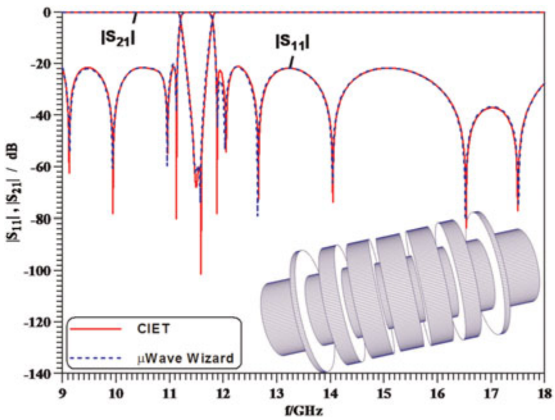

Fig. 7. Performance of a bandstop filter with seven TM_{110}-mode resonators; dimensions cf. Table 1.

very similar resonance frequency must be cascaded. The performance of such a seven-resonator filter is shown in Fig. 7. The 20 dB return loss bandwidth extends up to 11.14 GHz and beyond 11.86 GHz; the 20 dB rejection band lies between 11.3 and 11.7 GHz with more than 60 dB attenuation between 11.46 and 11.59 GHz.

A lowpass filter is obtained by following the same design principle as for the bandstop filter. However, the individual notch sections have to be initially designed for different frequencies to cover the entire stopband towards higher frequencies. This leads to a design that, contrary to the ones shown previously, is asymmetric in axial direction, but still maintains rotational symmetry. The inset in Fig. 8 depicts a lowpass filter formed by nine TM_{110}-mode cavities, each of which contributes to one of the nine notch frequencies shown between 14.4 and 18 GHz in Fig. 8. The level of attenuation was set to 35 dB during optimization with a return loss of at least 20 dB in the passband from 9 to 14 GHz. As in previous examples, excellent agreement with results from the µWave Wizard is demonstrated.

IV. CONCLUSION

Novel designs of TM_{11}-mode filters in circular waveguide technology are presented. It is demonstrated that such filters possess a number of significant advantages to standard circular waveguide iris filters. TM_{11}-mode filters are smaller and do not suffer from a second passband within the frequency range of application. They allow for design flexibility with respect to lowpass, highpass, bandpass, and bandstop operation. All filter structures exhibit cross-sectional rotational symmetry and thus preserve the polarization of any input signal. Excellent agreement with the commercially available software package µWave Wizard validates the design approach. A tolerance analysis for the bandpass filter reveals dependencies comparable to other filters of comparable bandwidths. Structural dimensions of all filters are provided and can be scaled to different frequency bands.

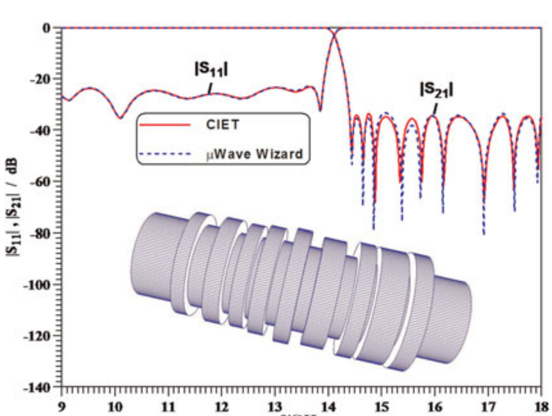

Fig. 8. Performance of a lowpass filter with nine TM_{110}-mode resonators; dimensions cf. Table 1.

REFERENCES

[1] Sun, W.; Balanis, C.A.: Analysis and design of quadruple-ridged waveguides. IEEE Trans. Microw. Theory Tech., **42** (1994), 2201–2207.

[2] Vanin, F.M.; Wollack, E.J.; Zaki, K.; Schmitt, D.: Polarization-preserving quadruple-ridge waveguide filter and four-fold symmetric transformer, in IEEE MTT-S Int. Microwave Symp. Digest, 2006, 127–140.

[3] Zhang, H.Z.: A wideband orthogonal-mode junction using a junction of a quad-ridged coaxial waveguide and four ridged sectoral waveguides. IEEE Microw. Wirel. Compon. Lett., **12** (2002), 172–174.

[4] James, G.L.; Clark, P.R.; Greene, K.J.: Diplexing feed assembly for application to dual-reflector antennas. IEEE Trans. Antennas Propag., **51** (2003), 1024–1029.

[5] Thiart, H.A.; Rambabu, K.; Bornemann, J.: Prototype design of a dual-band dual-polarization Ku/Ka-band feed. Proc. Eur. Microw. Assoc., **2** (2006), 318–325.

[6] Amari, S.; Bornemann, J.: Design of polarization-preserving circular waveguide filters with attenuation poles, Microw. Opt. Technol. Lett., **31** (2001), 334–336.

[7] Olver, A.D.; Clarricoats, P.J.B.; Kishk, A.A.; Shafai, L.: Microwave Horns and Feeds, IEEE Press, New York, 1994.

[8] Buckley, M.J.; Stein, D.A.; Vernon, R.J.: A single-periodic TE02-TE01 mode converter in a highly overmoded circular waveguide. IEEE Trans. Microw. Theory Tech., **39** (1991), 1301–1306.

[9] Amari, S.; Bornemann, J.: Design of mode converters using the coupled-integral-equations technique, in Proc. AP2000 Millennium Conf. Antennas Propagation, vol. 3A1, 2000, 4pp.

[10] Atia, A.E.; Williams, A.E.: New types of waveguide bandpass filters for satellite transponders. COMSAT Tech. Rev., **1** (1971), 21–43.

[11] Moretti, S.; Alessandri, F.; Sorrentino, R.: Field theory design of a novel circular waveguide dual-mode filter. Eur. Microw. Conf., **25** (1995), 779–783.

[12] Rosenberg, U.; Schneider, M.: Power splitting transition for circularly polarized feed networks. IEEE Microw. Wirel. Compon. Lett., **10** (2000), 307–309.

[13] Amari, S.; Rosenberg, U.; Bornemann, J.: Singlets, cascaded singlets and the non-resonating node model for advanced modular design of elliptic filters. IEEE Microw. Wirel. Compon. Lett., **14** (2004), 237–239.

[14] Lee, C.S.; Lee, S.W.; Chuang, S.L.: Plot of modal field distribution in rectangular and circular waveguides. IEEE Trans. Microw. Theory Tech., **39** (1985), 271–274.

[15] Bornemann, J.; Yu, S.Y.: Circular waveguide TM11-mode resonators and their application to polarization-preserving bandpass and quasi-highpass filters, in German Microwave Conf. (GeMiC), 2010, 202–205.

[16] Matthaei, G.; Young, L.; Jones, E.M.T.: Microwave Filters, Impedance Matching Networks, and Coupling Structures, Artech House, Boston, 1980.

[17] Uher, J.; Bornemann, J.; Rosenberg, U.: Waveguide Components for Antenna Feed Systems. Theory and CAD, Artech House, Norwood, 1993.

[18] Rosenberg, U.; Amari, S.; Bornemann, J.: Inline TM_{110}-mode filters with high design flexibility by utilizing bypass couplings of non-resonating $TE_{10/01}$ modes. IEEE Trans. Microw. Theory Tech., **51** (2003), 1735–1742.

[19] Madsen, K.; Schaer-Jacobsen, H.; Voldby, J.: Automated minimax design of networks. IEEE Trans. Circuits Systems, **22** (1975), 791–796.

[20] Bornemann, J.; Rosenberg, U.; Amari, S.; Vahldieck, R.: Tolerance analysis of bypass-, cross- and direct-coupled rectangular waveguide bandpass filters. IEE Proc., Microw. Antennas Propag., **152** (2005), 167–170.

[21] Rosenberg, U.; Amari, S.; Bornemann, J.; Vahldieck, R.: Compact pseudo-highpass filters formed by cavity and iris resonators. Eur. Microw. Conf., **34** (2004), 985–988.

Jens Bornemann received the Dipl.-Ing. and the Dr.-Ing. degrees, both in electrical engineering, from the University of Bremen, Germany, in 1980 and 1984, respectively. From 1984 to 1985, he was a consulting engineer. In 1985, he joined the University of Bremen, Germany, as an assistant professor. Since April 1988, he has been with the Department of Electrical and Computer Engineering, University of Victoria, Victoria, BC, Canada, where he became a professor in 1992. From 1992 to 1995, he was a fellow of the British Columbia Advanced Systems Institute. In 1996, he was a visiting scientist at Spar Aerospace Limited (now MDA Space), Ste-Anne-de-Bellevue, Québec, Canada, and a visiting professor at the Microwave Department, University of Ulm, Germany. From 1997 to 2002, he was a co-director of the Center for Advanced Materials and Related Technology (CAMTEC), University of Victoria. From 1999 to 2002, he served as an associate editor of the *IEEE Transactions on Microwave Theory and Techniques* in the area of Microwave Modeling and CAD. In 2003, he was a visiting professor at the Laboratory for Electromagnetic Fields and Microwave Electronics, ETH Zurich, Switzerland. From 1999 to 2008, he served on the Technical Program Committee of the *IEEE MTT-S International Microwave Symposium*. He has coauthored *Waveguide Components for Antenna Feed Systems, Theory and Design* (Artech House, 1993) and has authored/coauthored more than 220 technical papers. His research activities include RF/wireless/microwave/ millimeter-wave components and systems design, and field-theory-based modeling of integrated circuits, feed networks, and antennas. Dr. Bornemann is a registered professional engineer in the Province of British Columbia, Canada. He is a fellow IEEE and a fellow of the Canadian Academy of Engineering.

Seng Yong Yu received the B.Sc. degree from the Department of Physics, East China Normal University, Shanghai, China in 1985, the M.Sc. degree from the Department of Physics, Kumamoto University, Kyushu, Japan in 1996 and the Ph.D. degree from the Department of Electrical and Computer Engineering, University of Victoria, Victoria, BC, Canada, in 2008. From 1985 to 1994, he worked as an electronic engineer in the Shanghai Shipbuilding Industry Co. From 1994 to 1997, he was an assistant research engineer in the Physics Laboratory of Kumamoto University, where he was mainly engaged in the design and development of cryogenic laser devices for spectroscopy. Since January 2009, he is a postdoctoral fellow at the University of Victoria. His research interests include numerical analysis and techniques in electromagnetics, modeling of guided-wave structures, computer-aided design, and efficient optimization using frequency domain simulation methods for various applications.